Measuring 511 keV photon interaction locations in three dimensions using 3-D position sensitive scintillation detectors

A. Vandenbroucke, F.W.Y. Lau, P.D. Reynolds, C.S. Levin
Dept. of Radiology, Stanford University, USA

I. Introduction

We are studying a novel scintillation detector design for 511 keV photons whereby individual interaction locations are precisely determined in all three dimensions. The concept is shown in Fig. 1. A 3-D position sensitive detector is formed by stacking layers of scintillation crystals coupled to position sensitive avalanche photodiodes (PSAPDs). Charge created by the PSAPDs is routed to subsequent electronics over a flexible circuit. In this paper, 511 keV photons enter the scintillation crystals from the top ('face-on'). A source could also be positioned so that annihilation radiation enters from the edge ('edge-on'). This multi-layer design enables direct measurement of each interaction of annihilation photons in all three dimensions. 'Depth-of-Interaction' is directly measured and does not need to be estimated as in many other designs, such as monolithic crystal designs or dual ended readout. In addition, a high light collection efficiency is obtained due to the large aspect ratio compared to more traditional designs where scintillation light is read out at the end of a long scintillation crystal element. Furthermore, the design enables dense crystal packing. Previously we have published the spatial resolution of these modules [1], and a dedicated multiplexing scheme [2]. This paper presents for the first time a measurements of a stack of these modules and thus a scintillation detector with 3-D positioning capabilities.

II. Methods

The detector module design is depicted in Fig. 2. Each module consists of two 8×8 arrays of $1 \times 1 \times 1$ mm^3 Lutetium-Yttrium Oxyothosilicate (LYSO) crystals coupled to two distinct (1×1cm^2) Position-Sensitive-Avalanche Photodiodes (PSAPDs, RMD inc), both mounted on the same flex circuit. The PSAPDs require a bias voltage of 1750 Volt and have a gain of about 1000. An alumina frame provides rigidity to the module and serves as an alignment structure for the crystal arrays. This dual LYSO-PSAPD module also features several holes for alignment and mounting purposes.

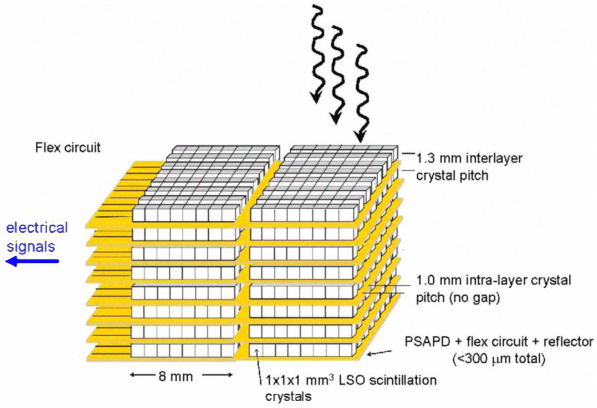

Fig. 1: Concept of the 3-D position sensitive scintillation detector used in this paper to measure photon interaction locations in three dimensions.

The flexible circuit is made out of liquid crystal polymer (LCP) because of its superior moisture properties compared to polyimide (Kapton). The two PSAPDs in a module are multiplexed to reduce the channel count. With multiplexing, 6 signal lines are used to readout 128 crystal pixels.

The experimental setup is shown in Fig. 3. A special mounting structure houses 4 dual modules. The structure is able to hold up to 8 dual modules. An intermediate flex circuit is connected to the modules to bring the signal to a routing board. From there, signals are routed over 30 cm long standard flat flexible cables (FFC) to a discrete board which houses AC-coupling capacitors. The discrete board also provides the bias voltage to the PSAPD chips and features signal conditioning resistors and capacitors to match the input dynamic range of the readout ASIC.

The discrete board connects to a readout board featuring a RENA-3 chip [3] (NOVA, Riverside, CA), ADCs and an FPGA. The RENA-3 chip houses 36 channels, each having a preamplifier, shaper and peak detection

A. Vandenbroucke is at the Department of Radiology, Stanford University. F.W.Y. Lau and P.D. Reynolds are at the Departments of Radiology and Electrical Engineering, Stanford University. C.S. Levin is at the Departments of Bioengineering, Electrical Engineering and Radiology at Stanford University. All authors are associated with the Molecular Imaging Program at Stanford.
Corresponding author: arnevdb@stanford.edu

U.S. Government work not protected by U.S. copyright

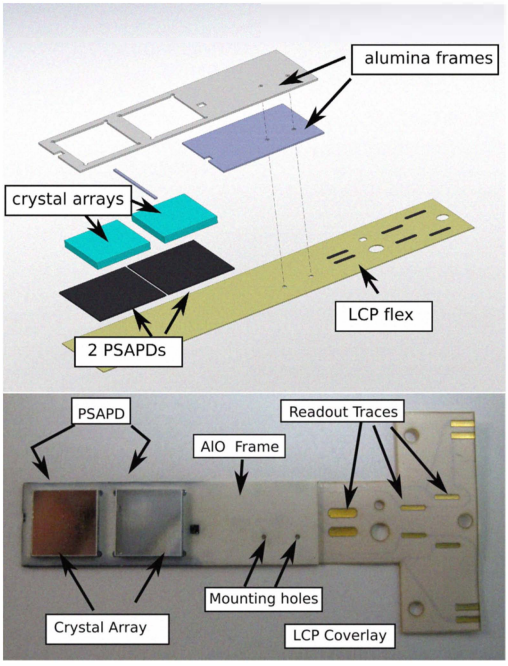

FIG. 2: Top: Schematic of a dual LYSO-PSAPD module. The bottom shows a photograph of a module used in this work.

circuitry. Digitized list-mode data is transferred to a PC using a USB cable.

Data was acquired using a ^{22}Na point source. The RENA-3 was triggered whenever the common of any of the 8 PSAPD units (4 dual modules) used in the setup crossed a certain threshold. Data was collected over several hours and no thermal regulation was used. All modules were biased at 1750 Volt.

Fig 4 shows the labeling of the 4 modules in the stack with respect to the incoming radiation. The nomenclature defined in this picture will be used throughout this manuscript.

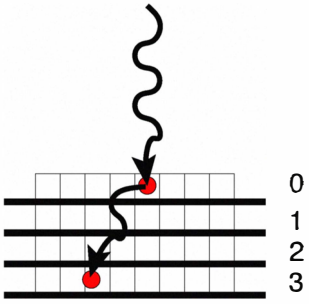

FIG. 4: Example of a multi-interaction event: A photon undergoes Compton scatter in module 0 and is photo-electrically absorbed in module 3.

III. RESULTS

A. *Energy resolution and crystal identification*

Fig. 5 shows a flood histogram for one LYSO-PSAPD unit as well as a global energy histogram. All 64 crystals in the flood histogram were identified by a peak searching algorithm. The global energy spectrum, depicted on the right in the same figure was obtained after correcting for light yield differences across the 8×8 array. A double Gaussian was fit to the photopeak. The width of both Gaussians was kept the same. The mean of these functions describe the photopeak and the X-ray escape peak respectively. An overall energy resolution of 10.8 ± 0.2 % FWHM at 511 keV was obtained. All other modules had a similar energy resolution.

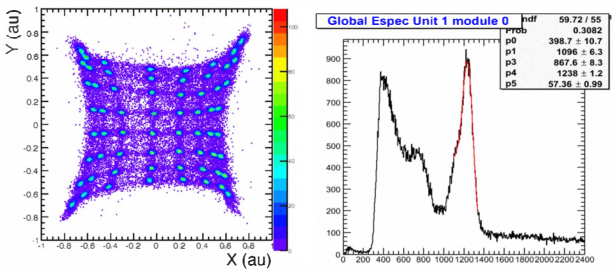

FIG. 5: Left panel shows a flood histogram of the crystal array mounted to module 0). Right shows an energy spectrum for the same array. Fit parameters of a Double Gaussian fit are indicated in the figure. $p1$ and $p4$ describe the X-ray escape and photopeak positions. $p5$ is the width of the Gaussian. $p0$ and $p3$ are parameters describing the amplitude of both Gaussians.

B. *Photoelectric events and cross talk*

3-D interaction positioning requires low electronic cross talk between detector layers. Therefore, we investigated inter-layer cross-talk on an event by event basis by recording the number of hits registered in the neighboring modules when one module detects a 511 keV photo-electric event. Fig. 6 shows the results of the analysis. Focusing on photoelectric interactions in Module 1 (about 1.3 mm deep within the 4-layer detector), all 64 crystals are identified in Module 1, whereas the other modules register very few hits (2.5 %, 1.9 % and 0.5 % for modules 0,2,3 respectively), indicating a limited amount of cross-talk. This data indicates that we can identify interaction locations in three dimensions.

Figure 7 shows the entire energy spectrum for module 2 plotted on a log-scale. The photopeak around 511 keV is clearly visible. Higher energy events correspond to the detection of the 1.2 MeV photon that is emitted simultaneously upon positron decay of a ^{22}Na nucleus. The blue histogram shows the hits registered simultaneously in the same module 2 when an photopeak event is registered in module 1. Cross talk is about 2 orders of magnitude lower across the entire energy range.

Another way to look at the ability of identifying single layers within a stack is to plot the energy deposited in

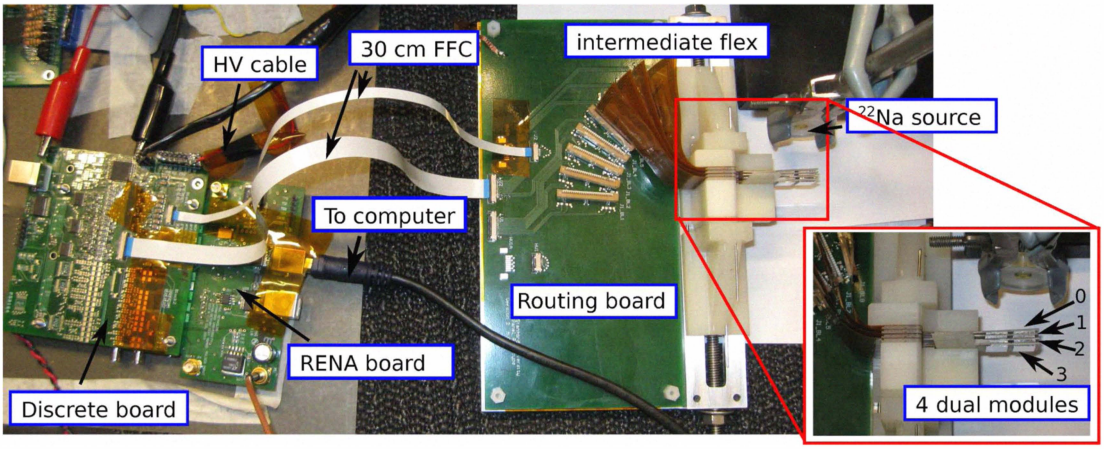

FIG. 3: Top view of the setup used in this paper. Various components are indicated in the figure.

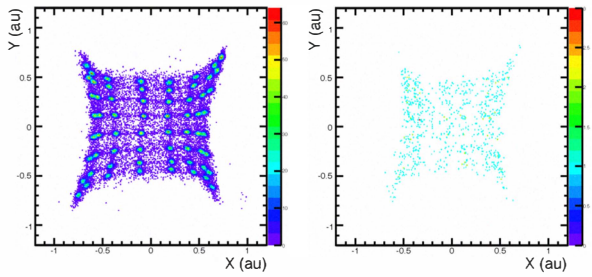

FIG. 6: Cross talk analysis. 64 crystals are identified in module 1 in the left panel. The right panel shows the hits in module 2 that are simultaneously registered when module 1 triggers. The limited number of hits in module 2 is evidence for low cross talk.

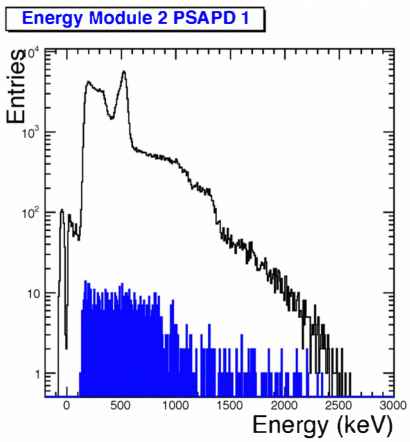

FIG. 7: The blue histogram represents cross talk hits registered in module 2 when a photopeak event is registered in module 1. The black histogram shows the energy spectrum of all hits in module 2. Note the log scale on the y-axis.

module 0 versus the energy deposited in module 1, as depicted in Figure 8. The z-scale is logarithmic on the figure. On the x and y axis we see projections of standard energy spectra for module 0 and module 1 respectively. A photopeak is distinguished in both spectra. We see only few noise hits, which all appear to be uncorrelated, except for an anti-correlation band corresponding to multiple-interaction events which will be discussed in the next section. The energy threshold is also visible in the figure.

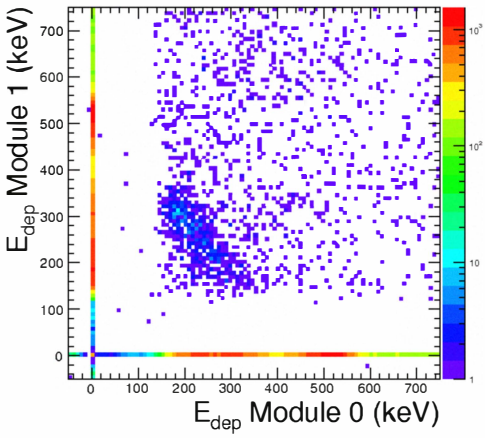

FIG. 8: Cross talk analysis. The energy deposition in module 0 versus the energy deposition in module 1. The z-axis is logarithmic. Apart from the band corresponding to multiple photon interactions, no correlated noise is observed.

C. Photon events with two interactions

Figure 8 suggests we should be able to distinguish multi-interaction events, in particular two photon events, where a photon Compton scatters in a first layer and is absorbed in a subsequent layer by a photoelectric interaction. Figure 9 shows the energy deposited in module 1 and module 2 for those events which had less than 400 keV of energy deposited in a single layer. We see that in general the energy deposited in module 1 is smaller than the energy deposited in module 2,

corresponding to forward Compton scatter followed by photoelectric absorption.

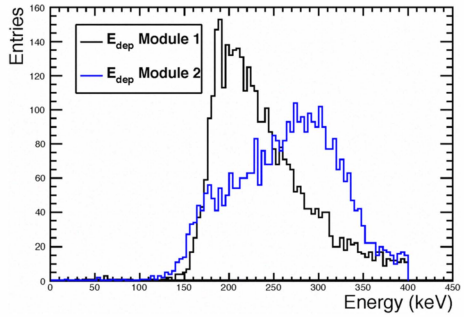

FIG. 9: Energy deposited in module 1 (black histogram) and energy deposited in module 2 (blue histogram) for those events with less than 400 keV energy deposited in module 1 or module 2. The lower average energy deposited in module 1 versus module 2 corresponds to forward Compton scatter from module 1 into module 2.

Adding the energy depositions in two layers, we obtain a picture like Figure 10. We see the sum of the energy deposited in module 0 and module1, module 0 and module2 and module 0 and module 3. In all cases we see a peak appearing around 511 keV, corresponding to the total energy of the photon. The width of the peak is 19.5 ± 0.7 % FWHM. We also see that there are fewer events in the M0+M3 combination than the M0+M2 and M0+M1 combination, in agreement with what is to be expected.

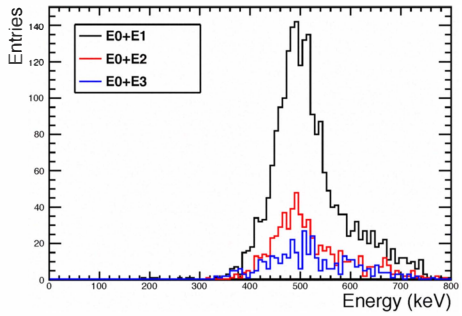

FIG. 10: Sum of the energy deposited in two layers (layer 0 and layer 1, layer 0 and layer 2, and layer 0 and layer 3). The total energy deposited in both layers adds up to a mean of 511 keV.

IV. CONCLUSIONS

We present for the first time data obtained with a detector comprising multiple layers of dual LYSO-PSAPD modules. We achieved < 11 % FWHM energy resolution for single layer hits. Results show we are able to position multi-interaction photon events in three dimensions, with a direct measurement of the depth of each interaction. The energy deposition of these events adds up to 511 keV. The preliminary data presented in this paper is a first proof-of-concept of a 3-D position-sensitive scintillation detector.

ACKNOWLEDGMENTS

We wish to thank the following funding resources: NIH R01CA119056 and R01CA119056S1 (ARRA), UC Breast Cancer Research Program 16GB-0060, ARCS Scholarship, and DOD BC094158. We also thank Richard Farrell from RMD.

REFERENCES

[1] A. Vandenbroucke, A. M. K. Foudray, P. D. Olcott, and C. S. Levin, "Performance characterization of a new high resolution PET scintillation detector," *Phys. Med. Biol.*, vol. 55, no. 19, pp. 5895–5911, 2010.

[2] F. W. Y. Lau, A. Vandenbroucke, P. D. Reynolds, P. D. Olcott *et al.*, "Analog signal multiplexing for PSAPD-based PET detectors: simulation and experimental validation," *Phys. Med. Biol.*, vol. 55, p. 7149, 2010.

[3] S. Kravis, T. Tümer, G. Visser, D. G. Maeding *et al.*, "A multichannel readout electronics for nuclear application (RENA) chip developed for position sensitive solid state detectors," *Nucl. Instr. Meth. A*, vol. 422, pp. 352–356, 1999.